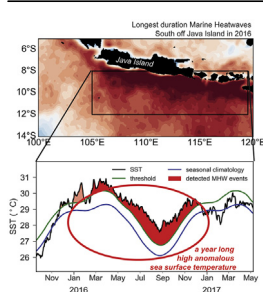




Research article

Marine heatwaves of sea surface temperature off south JavaMochamad Riza Iskandar ^{a,*}, Mochamad Furqon Azis Ismail ^a, Taslim Arifin ^b, Handy Chandra ^b^a Research Center for Oceanography, National Research and Innovation Agency of Indonesia, Jakarta, Indonesia^b Marine Research Center, Ministry of Marine Affairs and Fisheries, Republic of Indonesia, Jakarta, Indonesia**HIGHLIGHTS**

- First assessment of MHWs south off Java using high-resolution satellite SST products.
- The most intense and longest MHWs events are identified in 1998 and 2016.
- Record-breaking MHWs occurred during strong El Niño and weakened monsoon wind.

GRAPHICAL ABSTRACT**ARTICLE INFO****Keywords:**

Marine heatwaves
Sea surface temperature
South Java
Satellite

ABSTRACT

The frequency of marine heatwaves (MHWs) events has been rising globally in recent years, and this trend is expected to continue in the region off the coast of south Java Island. These oceanic extreme events may have the potential to devastate marine habitats, ecosystems and fisheries. This paper characterized MHWs off south Java from 1982 to 2019 using satellite-observed sea surface temperature. The aim of this study was to examine the dynamics of MHWs in one of Indonesia's most important fisheries hotspots, located in the southeast of the tropical Indian Ocean. We have identified two strong MHWs events in 1998 and 2016, both of which started in the austral winter months. Both events were lasted through the spring before dissipating in the early austral winter. These intense MHWs were likely related to a strong El Niño and decreased monsoon activity.

1. Introduction

In the atmosphere, a heatwave is defined as a period of unusually hot weather that lasts for an extended period of time (Coumou and Rahmstorf, 2012; Schär et al., 2004). This occurrence has a significant impact on a variety of areas, including agriculture, water resources, energy demand, human health, and socio-economic over a wide range (Radinović and Ćurić, 2012; Schär et al., 2004). A similar occurrence occurs in the ocean and is known as marine heatwaves (MHWs) (Hobday et al., 2016). MHWs defined as a prolonged discrete anomalously high sea surface temperature (SST) in a particular location (Hobday et al., 2016, 2018).

MHWs have been observed in many locations in the world ocean and can occur both in summer and winter-known as “winter warm-spells” (Atkinson et al., 2020; Hobday et al., 2018; Oliver et al., 2018a).

The influence of MHWs on the marine environment and ecosystem changes is enormous (Oliver et al., 2019; Wernberg et al., 2016). It has been reported that MHWs can lead to coral bleaching (Hughes et al., 2017), decrease in surface chlorophyll content (Bond et al., 2015), loss of kelp forests (Wernberg et al., 2016), mangrove mortality (Sippo et al., 2018), mass death of marine invertebrates due to thermal stress (Oliver et al., 2017), and fishery or aquaculture closures (Caputi et al., 2016; Oliver et al., 2017). Aside from biological concerns, this event is thought

* Corresponding author.

E-mail address: iskandarriza@ymail.com (M.R. Iskandar).

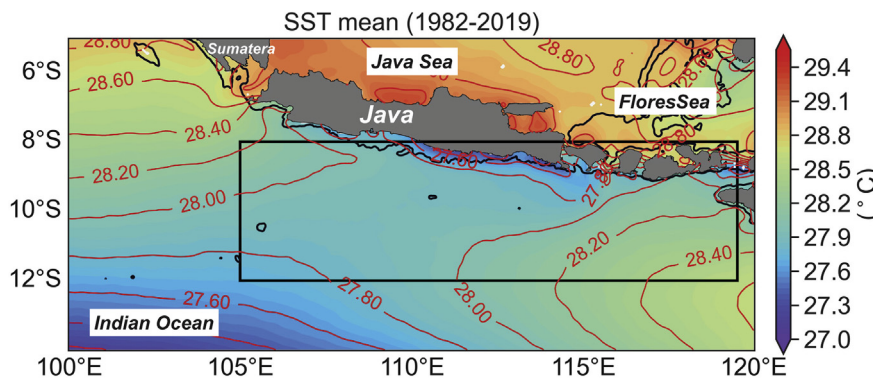


Figure 1. Map of the study site off south of Java. Shade color represents the mean of sea surface temperature (SST) over the period of 1982–2019. Black contour represents the isobath at 500 m depth. The red contour represents SST mean every 0.2 °C. Box region represents the area for the calculation of the time series of MHWs properties in the site off south of Java for the calculation of the MHW properties shown in Figures 4, 5, 6, and 7.

to have impacted the country's socio-economic and political conditions (Oliver et al., 2018a). Thus, characterizing this phenomenon is critical, and much attention must be paid to the consequences and impacts of this event.

It is expected that the intensity and frequency of MHWs will intensify under anthropogenic climate change (Frölicher et al., 2018; Oliver et al., 2018a, 2018b). In the past few decades, MHWs have become persistent, more frequent, intense, and this trend will further intensify under global warming (Frölicher et al., 2018). MHWs can be caused by a lot of factors. The most common drivers of MHWs include ocean currents which can accumulate warm water and air-sea heat flux, the wind that affects the warming of MHWs, and climate mode like El Niño (Frölicher et al., 2018; Holbrook et al., 2019; Sen Gupta et al., 2020). The first notable events of MHWs occurred in the northern Mediterranean in 2003 (Sparnocchia et al., 2006), followed by MHWs in the Northwest Atlantic in 2012 (Chen et al., 2014), the Northeast Pacific 2013–2015 (Bond et al., 2015; Di Lorenzo and Mantua, 2016), along the western coast of Australia in 2011

(Pearce and Feng, 2013), and tropical Australia in 2016 (Benthuyzen et al., 2018).

The Indonesian Sea is a choke point in the global thermohaline circulation (Gordon, 1986). This region may serve as a global warming hotspot that transfers excess heat as well as freshwater flux from the Pacific Ocean to the Indian Ocean (Hu and Sprintall, 2017). Despite the fact that the increase of MHWs over the centuries and the detection of MHWs in various parts of the world has been widely reported (Bond et al., 2015; Caputi et al., 2016; Di Lorenzo and Mantua, 2016; Frölicher et al., 2018; Holbrook et al., 2019), this extreme ocean temperatures event in the Indonesian Seas have not been fully explored. Given that the Indonesian Sea has the highest marine biodiversity and the world's fourth-largest population, studying the MHWs pattern is a significant issue in this region (Smale et al., 2019).

The southern coastal ocean of Java Island (SJI, Figure 1) is a highly dynamic region characterized by high mesoscale eddies activity (Azis Ismail et al., 2021), reversed south Java current (Sprintall et al., 2010),

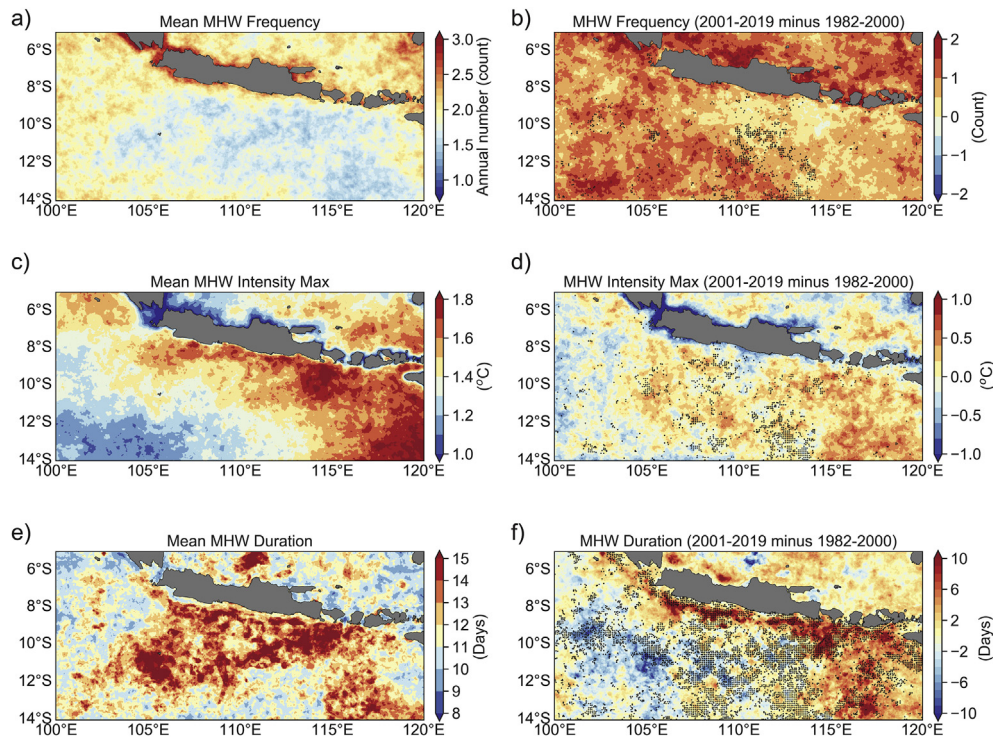


Figure 2. Mean of MHWs properties. a) frequency, c) intensity maximum, and e) duration. Mean over the 1982–2019 period. b), d), and f) difference between the 1982–2000 and 2001–2019 periods. The stippled areas in b, d and f denote significant trends ($p > 0.05$).

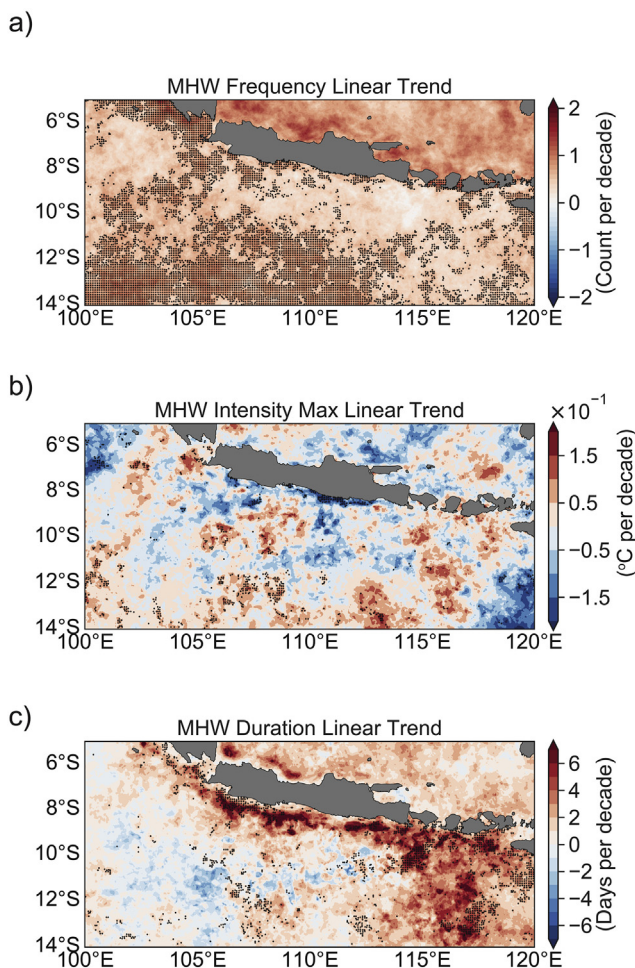


Figure 3. The linear trend of MHWs properties over the 1982–2019 period. a) frequency, b) intensity maximum, and c) duration. The stippled areas represent significant linear trend ($p > 0.05$).

intraseasonal equatorial Kelvin waves (Pujiyana and McPhaden, 2020), the Indian Ocean Dipole (IOD) onset (Saji et al., 1999), and seasonal upwelling (Susanto et al., 2001). The SJI is known as one of the fisheries hotspots for commercial tuna species (Andriyono, 2018; Syahputra et al., 2020). According to Oliver et al. (2018a, 2018b), the southern area off Java Island is one of the places where the intense MHWs occur in the Indonesian Seas. The MHWs that frequently occurs in this region could affect the marine species life that influences their tolerances due to heat stress during MHWs events. Up until now, there is no detailed description of the MHWs in the SJI. Therefore, the aim of this study is to investigate the MHWs dynamics and quantify their metrics in order to provide information and guidance for fisheries management in one of the country's most significant fisheries zones (Andriyono, 2018; Lumban-Gao et al., 2021; Suadi and Kusano, 2019; Syahputra et al., 2020).

2. Materials and methods

2.1. Satellite data

The high-resolution SST dataset used in this study is daily Operational SST and Sea Ice Analysis (OSTIA) on 0.05° spatial grids (Donlon et al., 2012) obtained from the Copernicus Marine Environment Monitoring Service (CMEMS). We used OSTIA data from 1 January 1982 to 31 December 2019. Time series of SST in the box area in the south of Java Island is generated by spatially averaging SST over the region. The box region in the south coast of Java is located in $105^{\circ}\text{--}115^{\circ}\text{E}$ and $7^{\circ}\text{--}11^{\circ}\text{S}$.

The area of interest (AOI) in this study is located in the $100^{\circ}\text{--}119.5^{\circ}\text{E}$ and $5^{\circ}\text{--}14^{\circ}\text{S}$ as shown in Figure 1. Niño 3.4 Index ($170^{\circ}\text{W}\text{--}120^{\circ}\text{W}$, $5^{\circ}\text{S}\text{--}5^{\circ}\text{N}$) used in this study is based on daily SST Optimum Interpolation version 2 accessed from <https://climexp.knmi.nl/getindices.cgi>, accessed on 21 July 2021. The Dipole Mode Index (DMI) is based on daily Reynolds Optimal Interpolation version 2 SST analysis accessed from the National Oceanic and Atmospheric Administration (NOAA) webpage (<https://stateoftheocean.osmc.noaa.gov/sur/ind/dmi.php>, accessed on 21 July 2021). Australian monsoon index used in this paper is the normalized number based on calculation from Kajikawa et al. (2010) using National Center for Environmental Prediction/National Center for Atmospheric Research (NCEP/NCAR) reanalysis that can be accessed from Asia-Pacific Data-Research Center (<http://apdrc.soest.hawaii.edu/projects/monsoon/seasonal-monidx.html>, accessed on 21 July 2021). Monthly 850 hPa averaged zonal (u) and meridional (v) wind velocity is also used to examine the atmospheric circulation over the study area. u and v velocity products are based on the reanalysis data from European Centre for Medium-Range Weather Forecasts (ECMWF) Reanalysis v5 (ERA5) (Hersbach et al., 2020) (<https://cds.climate.copernicus.eu/cdsapp#!/dataset/reanalysis-era5-single-levels-monthly-means?tab=form>, accessed on 20 October 2021).

2.2. MHW detection

The MHWs are detected by identifying the periods when daily SST is above the threshold for at least five days sequentially (Hobday et al., 2016). Two events with a gap of fewer than 3 days are examined as a single event. The threshold is defined as seasonally varying 90th percentile. Similar to Hobday et al. (2016), the 90th percentile and climatological mean for each day of the year are calculated by using the daily SST within an 11-day window centered on a certain day and then smoothed by applying a 31-day moving average. The 11-day window and 31-day moving average are selected to establish an adequate sample size for percentile calculation and smooth climatology (Hobday et al., 2016, 2018; Oliver et al., 2017, 2018a, 2018b, 2019, 2021; Schlegel et al., 2017).

MHWs have metrics to describe the properties. The metrics considered in this study include duration (times between start and end day of MHWs event), and maximum intensity (maximum SST anomaly over MHWs duration). We then calculate the time series of annual average duration, annual maximum intensity, and frequency (number of MHWs events in each year). From the annual MHWs metrics that were calculated, we present differences in the mean value between two-time slices at 1982–2000 and 2001–2019. We also present a linear trend of the metrics at each location following the method from Oliver et al. (2018a, 2018b). Following the approach by Hobday et al. (2018), MHWs are classified as moderate, strong, severe, or extreme events by the local difference between the climatological mean and the threshold used to recognize MHWs (climatological 90th percentile). This difference can be estimated at each spatial-temporal point of an MHWs event based on the intensity measurement. Due to the lack of direct field measurements, this study is limited to detecting MHWs only using satellite data. Several other studies (e.g. Carvalho et al., 2021; Mawren et al., 2021; Miyama et al., 2021) identified MHWs by using SST from satellite products and drawing general conclusions based on those limited direct temperature measurements.

3. Results and discussion

Figure 2a, c, and e represent the long-term mean of MHWs metrics in the study region. Metrics shown in this figure are intensity maximum, duration, and frequency of the events. According to Figure 2a, the frequency of MHWs ranged from one to three events per year, depending on location. The highest frequency is found in the surrounding areas of Java and Sumatera Islands near the coastlines (outside AOI). The area from the Java Sea to the Flores Sea (outside AOI) experiences two MHWs per year

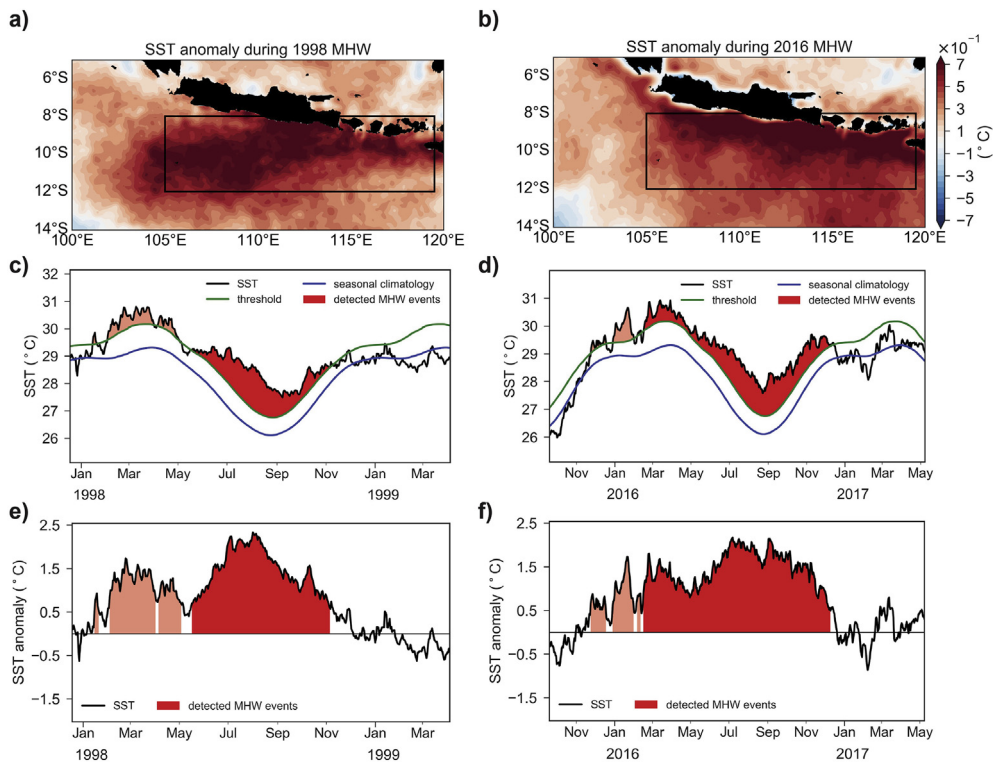


Figure 4. Mean of SST anomaly on the two MHWs during a) largest intensity maximum in 1998 and b) longest duration in 2016. c) Daily SST ($^{\circ}\text{C}$): OSTIA (black), threshold (green), and 1982–2019 climatology (blue) averaged over the area of interest off south Java Island in the box region during MHWs event in c) 1998 and d) 2016. (e) SST anomalies averaged over the box region during MHW events in e) 1998 and f) 2016.

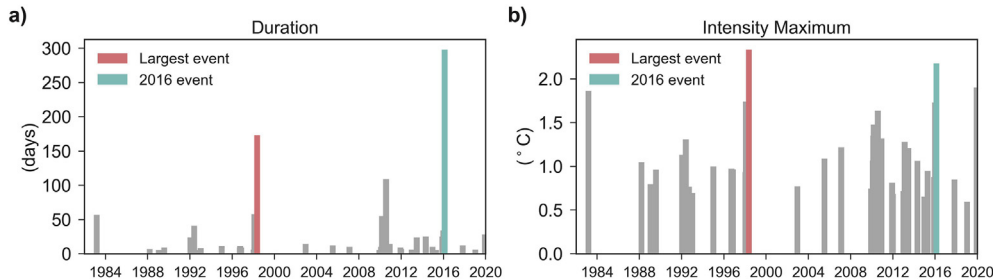


Figure 5. (a) Duration and (b) intensity maximum for all MHWs events on record start from 1982 in the box region in Figure 1. The red bar represents the largest MHW event based on the highest intensity maximum in 1998, and the blue bar represents the MHW event based on the longest duration in 2016.

on average, with the most notable exception being the area of SJI, which has fewer than two MHWs per year.

The maximum intensity of MHWs varies across spatial locations (Figure 2c). The location with the highest frequency of MHWs (Figure 2a), i.e. outside AOI in the region off the coast of north Java and Sumatera Islands, has the lowest intensity (Figure 2c). Meanwhile, high-intensity hotspots ($>1.4\text{ }^{\circ}\text{C}$) occur in the region off the coast of south Java Island (Figure 2c), where the MHWs occur with the lowest annual frequency (Figure 2a). The second high-intensity areas are found in the outer AOI near the coast of Australia ($>1.6\text{ }^{\circ}\text{C}$) and the Flores Sea ($1.4\text{--}1.7\text{ }^{\circ}\text{C}$), which is consistent with Benthuysen et al. (2018), who discovered the largest MHWs event in the Indo-Australia basin. The mean duration of MHWs varied across the AOI (Figure 2e). The longest duration of over 13 days is distributed spatially off south Java, while other regions are typically characterized by events of 8–10 days, with the exception of a small region in the Java Sea (outside AOI) around 110°E with up to 13-day mean durations.

Figure 2b, d, and f show the differences in MHWs metrics between the two time periods of 1982–2000 and 2001–2019. Significant positive

trends ($p > 0.05$) in MHWs frequency and intensity maximum are only noticed in a few areas off south Java (Figure 2b, d), while significant positive trends ($p > 0.05$) in MHWs duration are found in most of the region of the SJI (Figure 2f). MHWs frequency is likely to increase across all areas of interest. The largest increase occurred outside the AOI in the Java Sea and Flores Sea (>2 annual events). More moderate increases were observed in the Indian Ocean, including off the coast of south Java Island (1–2 annual events). There is no evidence of a decreases in the frequency of MHWs in any of the regions, indicating that MHWs have become more prominent in the recent decade. The intensity of MHWs is expected to increase in the Indian Ocean between 1982 and 2019, most notably on the eastern side of the AOI, as shown in Figure 2d, with a $1\text{ }^{\circ}\text{C}$ increase in temperature. Reduced MHWs intensity can be found on the western side of the AOI in the Indian Ocean, most notably along the north coast of Java and Sumatera Islands. Between 1982 and 2019, the duration of MHWs in the eastern part of the AOI and along the southern coast of Java Island increased by up to 10 days (Figure 2f).

To better understand the temporal changes of MHWs, we use the expected trends in MHWs properties at each coordinate, as described by

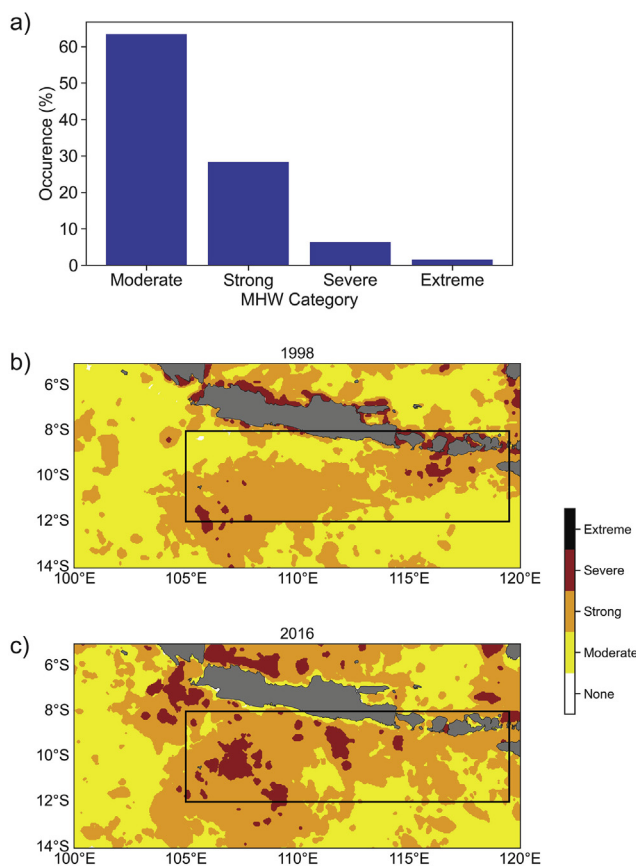


Figure 6. (a) Frequency distribution of MHWs in each category in the area of interest off south Java Island over the time period 1982–2019. Map locating maximum MHWs category occurrences for years (b) 1998, and (c) 2016. The black rectangle region is the area of interest.

[Oliver et al. \(2018a\)](#). The findings show that the frequency of MHWs is likely to increase in all the regions ([Figure 3a](#)) which implies MHWs occur regularly. Significant positive trends ($p > 0.05$) of MHWs frequency are found nearly across the entire area. However, there are less significant positive trend ($p > 0.05$) in MHWs intensity maximum and duration ([Figure 3b, c](#)). The linear trends of MHW duration patterns also show that the SJI has a positive trend, and it is shown as the largest trend among all regions ([Figure 3c](#)). Meanwhile, the maximum intensity pattern is intermittent, alternating between positive and negative trends ([Figure 3b](#)). From the metrics and trend of MHWs shown in Figures 2 and 3, the SJI is the place where high intensity and long duration of MHWs occur. This could indicate that MHWs are common in this area, and their presence could have an impact on the sensitive marine species.

To examine the strongest event of MHWs in this region, we present a time series of MHWs over a spatially averaged area of the SJI, as shown in [Figure 4](#). By using daily time series that averaged spatially off south Java Island ([Figure 4a](#)), we found that there are a greatest continuous MHWs from 17 May 1998 to 5 November 1998 ([Figure 4c, e](#)) based on the largest intensity maximum. There is a spatially distributed high SST anomaly during the MHWs event in 1998 ([Figure 4a](#)) that has a large anomaly of over 0.7°C . According to the MHWs metrics, this event has a duration of 173 days, a maximum intensity of 2.34°C , and a mean intensity of 1.49°C . This event showed the second-longest duration ([Figure 5a](#)) and the largest MHWs intensity on the record in the SJI ([Figure 5b](#)).

According to metrics of MHWs in the SJI, there is another continuous MHWs event in 2016 with the longest duration ([Figure 5a](#)). Despite the fact that the intensity maximum of MHWs in 2016 was not the highest of the MHWs recorded, the intensity maximum in 2016 was relatively high,

hovering around 2°C ([Figure 5b](#)). It is the second-largest intensity maximum among MHWs events recorded since 1982 ([Figure 5b](#)). Looking at the SST anomaly distribution, there is a high SST anomaly distributed spatially during the MHWs event in 2016. This high SST anomaly is also observed further west outside the AOI, reaching off the coast of Sumatera Island ([Figure 4b](#)). Time series of SST spatially averaged over the region ([Figure 4b](#)) show that year 2016 is a warm year for the entire year on the record, beginning with the moderate MHWs in January 2016 and ending with extremely long duration MHWs in February 2016 ([Figure 4d, f](#)). The intense MHWs lasted 298 days, from 16 February to 9 December 2016, with a maximum intensity of 2.18°C and mean intensity of 1.47°C .

Comparing all MHWs that occurred in each spatial coordinate in the AOI from 1982 to 2019 reveals that 64 % of all MHWs across regions are Category I, 28 % are Category II, 6 % are Category III, and there are very few Category IV events ([Figure 6a](#)). [Hobday et al. \(2016\)](#) suggest that these MHWs categories may better reflect the sensitivity of biological systems in each region. However, spatial maps of the maximum annual MHW category ([Figure 6b](#)) indicate that during two of the strongest MHWs events, based on the highest intensity maximum in 1998 and the longest duration in 2016, a strong or greater intensity MHWs affected about 80% of the ocean surface in the SJI, with MHWs affecting the majority of the ocean surface during those years.

The two strongest MHWs in 1998 and 2016 began in the austral winter months, lasted through the austral spring before dissipating in the early austral winter, and coexisted after the strong El-Niño events ([Figure 7a and b](#)). The high SST anomalies in 1998 and 2016 coincided with the strongest El Niño events since 1997–1998 and 2015–2016, respectively ([Figure 7b](#)). The El Niño lasted for a whole year and disappeared in the austral autumn of the following year. As the El Niño weakened ([Figure 7b](#)), so did the DMI of the Indian Ocean. Nonetheless, the DMI is shown to have a positive peak during strong El Niño. As shown in [Figure 7c](#), the most negative DMI values persisted in the austral winter of 1998 and 2016 ([Figure 7c](#)), potentially leading to warming of the water in the eastern Indian Ocean.

In the Indo-Australian Basin, including the SJI, SST anomalies tend to change quickly from negative (in austral spring) to positive (in austral summer) and remain positive until at least the austral autumn ([Zhang et al., 2017](#)). As the El Niño dissipated, these warm anomalies continued to exist throughout the austral winter due to the capacitor effect ([Xie et al., 2009, 2016](#)). The Australian monsoon index is a good indicator of monsoonal rain across the Indo-Australian basin, but it is weak during El Niño years. During periods of strong El Niño, the Australian monsoon index is low, especially in early 1998 and 2016 ([Figure 7d](#)), which tends to reduce monsoon rainfall across the Indo-Australian basin, including the SJI.

[Figure 8](#) depicts the mean of 850-hPa atmospheric circulations over the southern part of the Maritime Continent during austral summer in December-January-February (DJF) to inspect the monsoonal wind circulation that weakens during two strong MHWs events. [Figure 8a, b](#) show the annual average of the wind circulation at 850 hPa from December to February in 1998 and 2016, respectively. While [Figure 8c, d](#) show the annual average of the wind circulation during weak and strong monsoon years from ERA5 reanalysis data. [Figure 8d](#) shows how the monsoon index from [Kajikawa et al. \(2010\)](#) distinguishes between weak and strong monsoon years. [Figure 8a, b](#) show that the atmospheric circulations in DJF are weakening in the SJI when compared to the atmospheric circulation pattern during strong monsoon years ([Figure 8d](#)). The magnitude of wind in 1998 is smaller than the pattern seen during weak monsoon years, as shown in [Figure 8c](#).

[Benthuysen et al. \(2018\)](#) discovered that intense MHWs event during 2015–2016 in northern Australia coexisted with strong El Niño that dissipated in austral autumn 2016, negative IOD, and a low Australian monsoon index. They suggest the atmospheric heat flux was unusually strong during the 2016 MHWs, which would have greatly warmed the upper ocean. El Niño causes regional warming trends across Australia

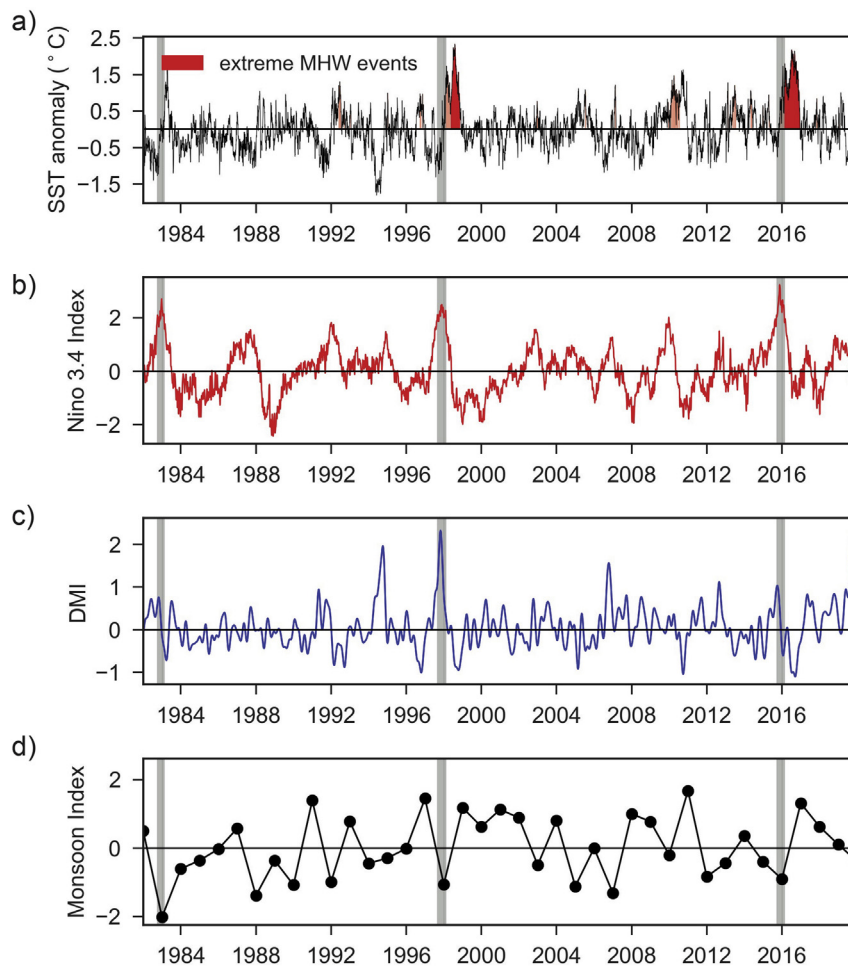


Figure 7. (a) Domain averaged (105° – 115°E and 7° – 11°S) SST anomalies based on a 1982–2019 climatology of OSTIA, (b) Niño 3.4 Index, (c) Dipole Mode Index (DMI), and (d) Australian monsoon index. Niño 3.4 Index is based on daily SST Optimum Interpolation version 2 (OI.v2) accessed from World Meteorological Organization (WMO). DMI is based on daily Reynolds OI.v2 SST analysis accessed from the National Oceanic and Atmospheric Administration (NOAA). Australian monsoon index is the normalized number based on calculation from Kajikawa et al. (2010) using National Centers for Environmental Prediction/National Center for Atmospheric Research (NCEP/NCAR) reanalysis. Butterworth low pass filter is applied to the weekly time series in Figure 6b and c. The vertical shaded grey bars denote the three strongest El Niños since 1982.

due to changes in atmospheric conditions, and El Niño years have been associated with a later onset and a weaker summer monsoon (Hung and Yanai, 2004; Redondo-Rodriguez et al., 2012). Our results are consistent with previous findings (e.g. Benthuysen et al., 2018; Oliver et al., 2018a) and it is anticipated that this study will be a starting step towards

planning the future of MHWs observation in the SJI. Following the characterization of MHWs using remotely-sensed SST in the SJI, a follow-up study could employ direct temperature measurements along the coast of south Java to provide more detailed information of MHWs dynamics in the region. However, our study is limited since no

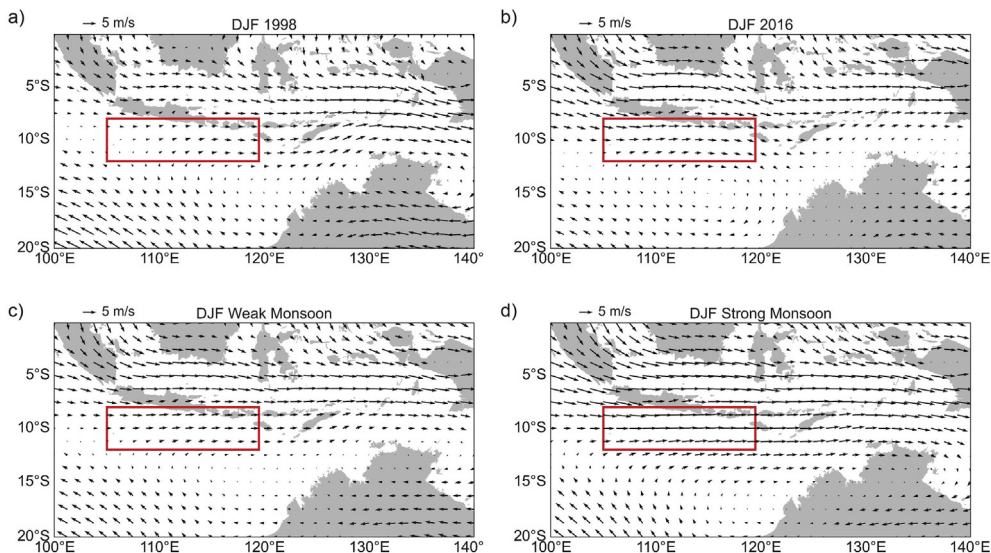


Figure 8. Mean 850 hPa horizontal winds of the Austral summer monsoon in a) 1998, b) 2016, c) weak monsoon, and d) strong monsoon years. Weak and strong monsoon years are separated based on the monsoon index by Kajikawa et al. (2010). The red rectangle is the Area of Interest (AOI) displayed in Figure 1.

continuous long-term in-situ records in the SJI. Therefore, future work will need to focus on minimizing the discussed uncertainties of this study. Nevertheless, a significant outcome from our study is that for the first time the MHWs dynamics and their metrics were characterized and quantified for the SJI.

4. Conclusion

We have characterized the MHWs properties for the SJI from 1982 to 2019 using daily time series remote-sensed and in-situ SST from OSTIA. MHWs properties are represented by the MHWs metrics including intensity maximum, duration, and MHWs frequency. We found that south Java Island is the location of the high intensity and long duration of MHWs with an annual frequency of less than two per year. We discovered that between 1982–2019, the spatial average of MHWs frequency and the average annual MHWs duration increased, along with the moderate increase in maximum intensity.

Examining daily SST time series allows characterizing MHWs events off the coast of south Java Island. We found that the year with the most intense MHWs in this region was 1998, whereas the year with the longest duration and relatively high intensity was 2016. These two strongest MHWs events began in the austral winter months of 1998 and 2016, lasted through the spring before disappearing in early austral winter. These MHWs are likely related to a strong El Niño and reduced monsoon activity. The drivers of these strong MHWs in this region does not examine in this study in detail and it could be investigated for future research. Further studies into MHWs could look into their impacts on the ecosystem, as well as the changes in other parameters such as salinity, nutrients, and so on.

Declarations

Author contribution statement

Mochamad Riza Iskandar, Mochamad Furqon Azis Ismail, Taslim Arifin & Handy Chandra: Conceived and designed the experiments; Performed the experiments; Analyzed and interpreted the data; Wrote the paper.

Funding statement

Mochamad Furqon Azis Ismail was supported by LIPI COREMAP-CTI 2021–2022 (17/A/DK/2021) and Alexander von Humboldt-Stiftung.

Mochamad Riza Iskandar was supported by National Research Foundation of South Korea.

Taslim Arifin and Handy Chandra were supported by Kementerian Kelautan dan Perikanan, Republik Indonesia.

Data availability statement

Data associated with this study has been deposited at Operational SST and Sea Ice Analysis (OSTIA).

Declaration of interests statement

The authors declare no conflict of interest.

Additional information

No additional information is available for this paper.

Acknowledgements

The authors are grateful to Copernicus Marine Environment Monitoring Service (CMEMS) for making the OSTIA products freely available. The authors also would like to thank Dr. Arnida L. Latifah for her assistance with the supercomputing service by the Indonesian Institute of

Sciences (HPC LIPI). Special thanks to the three reviewers for their constructive comments, which greatly improved our manuscript.

References

- Andriyono, S., 2018. Overview of Indonesia fisheries sector: Java and Bali island. *Int. J. Life Sci. Earth Sci.* 1, 39–48.
- Atkinson, J., King, N.G., Wilmes, S.B., Moore, P.J., 2020. Summer and winter marine heatwaves favor an invasive over native seaweeds. *J. Phycol.* 56, 1591–1600.
- Azis Ismail, M.F., Ribbe, J., Arifin, T., Taofiqurohman, A., Anggoro, D., 2021. A census of eddies in the tropical eastern boundary of the Indian ocean. *J. Geophys. Res. Ocean.* 126, 1–9.
- Benthuyzen, J.A., Oliver, E.C.J., Feng, M., Marshall, A.G., 2018. Extreme marine warming across tropical Australia during austral summer 2015–2016. *J. Geophys. Res. Ocean.* 123, 1301–1326.
- Bond, N.A., Cronin, M.F., Freeland, H., Mantua, N., 2015. Causes and impacts of the 2014 warm anomaly in the NE Pacific. *Geophys. Res. Lett.* 42, 3414–3420.
- Caputi, N., Kangas, M., Denham, A., Feng, M., Pearce, A., Hetzel, Y., Chandrapavan, A., 2016. Management adaptation of invertebrate fisheries to an extreme marine heat wave event at a global warming hot spot. *Ecol. Evol.* 6, 3583–3593.
- Carvalho, K.S., Smith, T.E., Wang, S., 2021. Bering Sea marine heatwaves: patterns, trends and connections with the Arctic. *J. Hydrol.* 600, 126462.
- Chen, K., Gawarkiewicz, G.G., Lentz, S.J., Bane, J.M., 2014. Diagnosing the warming of the Northeastern U.S. Coastal Ocean in 2012: a linkage between the atmospheric jet stream variability and ocean response. *J. Geophys. Res. Ocean.* 119, 218–227.
- Coumou, D., Rahmstorf, S., 2012. A decade of weather extremes. *Nat. Clim. Change* 2, 491–496.
- Di Lorenzo, E., Mantua, N., 2016. Multi-year persistence of the 2014/15 North Pacific marine heatwave. *Nat. Clim. Change* 6, 1042–1047.
- Donlon, C.J., Martin, M., Stark, J., Roberts-Jones, J., Fiedler, E., Wimmer, W., 2012. The operational sea surface temperature and sea ice analysis (OSTIA) system. *Remote Sens. Environ.* 116, 140–158.
- Förlacher, T.L., Fischer, E.M., Gruber, N., 2018. Marine heatwaves under global warming. *Nature* 560, 360–364.
- Gordon, A.L., 1986. Interocean exchange of thermocline water. *J. Geophys. Res.* 91, 5037.
- Hersbach, H., Bell, B., Berrisford, P., Hirahara, S., Horányi, A., Muñoz-Sabater, J., Nicolas, J., Peubey, C., Radu, R., Schepers, D., Simmons, A., Soci, C., Abdalla, S., Abellán, X., Balsamo, G., Bechtold, P., Biavati, G., Bidlot, J., Bonavita, M., De Chiara, G., Dahlgren, P., Dee, D., Diamantakis, M., Dragani, R., Flemming, J., Forbes, R., Fuentes, M., Geer, A., Haimberger, L., Healy, S., Hogan, R.J., Hölm, E., Janisková, M., Keeley, S., Laloyaux, P., Lopez, P., Lupu, C., Radnoti, G., de Rosnay, P., Rozum, I., Vamborg, F., Villaume, S., Thépaut, J.-N., 2020. The ERA5 global reanalysis. *Q. J. R. Meteorol. Soc.* 146, 1999–2049.
- Hobday, A., Oliver, E., Sen Gupta, A., Benthuyzen, J., Burrows, M., Donat, M., Holbrook, N., Moore, P., Thomsen, M., Wernberg, T., Smale, D., 2018. Categorizing and naming marine heatwaves. *Oceanography* 31.
- Hobday, A.J., Alexander, L.V., Perkins, S.E., Smale, D.A., Straub, S.C., Oliver, E.C.J., Benthuyzen, J.A., Burrows, M.T., Donat, M.G., Feng, M., Holbrook, N.J., Moore, P.J., Scannell, H.A., Sen Gupta, A., Wernberg, T., 2016. A hierarchical approach to defining marine heatwaves. *Prog. Oceanogr.* 141, 227–238.
- Holbrook, N.J., Scannell, H.A., Sen Gupta, A., Benthuyzen, J.A., Feng, M., Oliver, E.C.J., Alexander, L.V., Burrows, M.T., Donat, M.G., Hobday, A.J., Moore, P.J., Perkins-Kirkpatrick, S.E., Smale, D.A., Straub, S.C., Wernberg, T., 2019. A global assessment of marine heatwaves and their drivers. *Nat. Commun.* 10, 1–13.
- Hu, S., Sprintall, J., 2017. Observed strengthening of interbasin exchange via the Indonesian seas due to rainfall intensification. *Geophys. Res. Lett.* 44, 1448–1456.
- Hughes, T.P., Kerry, J.T., Álvarez-Noriega, M., Álvarez-Romero, J.G., Anderson, K.D., Baird, A.H., Babcock, R.C., Beger, M., Bellwood, D.R., Berkelmans, R., Bridge, T.C., Butler, I.R., Byrne, M., Cantin, N.E., Comeau, S., Connolly, S.R., Cumming, G.S., Dalton, S.J., Diaz-Pulido, G., Eakin, C.M., Figueira, W.F., Gilmour, J.P., Harrison, H.B., Heron, S.F., Hoey, A.S., Hobbs, J.-P.A., Hoogenboom, M.O., Kennedy, E.V., Kuo, C., Lough, J.M., Lowe, R.J., Liu, G., McCulloch, M.T., Malcolm, H.A., McWilliam, M.J., Pandolfi, J.M., Pears, R.J., Pratchett, M.S., Schoepf, V., Simpson, T., Skirving, W.J., Sommer, B., Torda, G., Wachenfeld, D.R., Willis, B.L., Wilson, S.K., 2017. Global warming and recurrent mass bleaching of corals. *Nature* 543, 373–377.
- Hung, C.-W., Yanai, M., 2004. Factors contributing to the onset of the Australian summer monsoon. *Q. J. R. Meteorol. Soc.* 130, 739–758.
- Kajikawa, Y., Wang, B., Yang, J., 2010. A multi-time scale Australian monsoon index. *Int. J. Climatol.* 30, 1114–1120.
- Lumban-Gaol, J., Siswanto, E., Mahapatra, K., Natih, N.M.N., Nurjaya, I.W., Hartanto, M.T., Maulana, E., Adrianto, L., Rachman, H.A., Osawa, T., Rahman, B.M.K., Permana, A., 2021. Impact of the strong downwelling (upwelling) on small pelagic fish production during the 2016 (2019) negative (positive) Indian Ocean Dipole events in the eastern Indian ocean off Java. *Climate* 9.
- Mawren, D., Hermes, J., Reason, C.J.C., 2021. Marine heatwaves in the mozambique Channel. *Clim. Dynam.*
- Miyama, T., Minobe, S., Goto, H., 2021. Marine heatwave of sea surface temperature of the Oyashio region in summer in 2010–2016. *Front. Mar. Sci.* 7, 1–12.
- Oliver, E.C.J., Benthuyzen, J.A., Bindoff, N.L., Hobday, A.J., Holbrook, N.J., Mundy, C.N., Perkins-Kirkpatrick, S.E., 2017. The unprecedented 2015/16 Tasman Sea marine heatwave. *Nat. Commun.* 8.
- Oliver, E.C.J., Benthuyzen, J.A., Darmaraki, S., Donat, M.G., Hobday, A.J., Holbrook, N.J., Schlegel, R.W., Sen Gupta, A., 2021. Marine heatwaves. *Ann. Rev. Mar. Sci.* 13, 313–342.

- Oliver, E.C.J., Burrows, M.T., Donat, M.G., Sen Gupta, A., Alexander, L.V., Perkins-Kirkpatrick, S.E., Benthuysen, J.A., Hobday, A.J., Holbrook, N.J., Moore, P.J., Thomsen, M.S., Wernberg, T., Smale, D.A., 2019. Projected marine heatwaves in the 21st century and the potential for ecological impact. *Front. Mar. Sci.* 6, 734.
- Oliver, E.C.J., Donat, M.G., Burrows, M.T., Moore, P.J., Smale, D.A., Alexander, L.V., Benthuysen, J.A., Feng, M., Sen Gupta, A., Hobday, A.J., Holbrook, N.J., Perkins-Kirkpatrick, S.E., Scannell, H.A., Straub, S.C., Wernberg, T., 2018a. Longer and more frequent marine heatwaves over the past century. *Nat. Commun.* 9, 1–12.
- Oliver, E.C.J., Lago, V., Hobday, A.J., Holbrook, N.J., Ling, S.D., Mundy, C.N., 2018b. Marine heatwaves off eastern Tasmania: trends, interannual variability, and predictability. *Prog. Oceanogr.* 161, 116–130.
- Pearce, A.F., Feng, M., 2013. The rise and fall of the “marine heat wave” off Western Australia during the summer of 2010/2011. *J. Mar. Syst.* 111–112, 139–156.
- Pujiana, K., McPhaden, M.J., 2020. Intraseasonal Kelvin waves in the equatorial Indian Ocean and their propagation into the Indonesian seas. *J. Geophys. Res. Ocean* 123, 1–18.
- Radinović, D., Čurić, M., 2012. Criteria for heat and cold wave duration indexes. *Theor. Appl. Climatol.* 107, 505–510.
- Redondo-Rodríguez, A., Weeks, S.J., Berkelmans, R., Hoegh-Guldberg, O., Lough, J.M., 2012. Climate variability of the great barrier reef in relation to the tropical Pacific and El Niño-southern oscillation. *Mar. Freshw. Res.* 63, 34–47.
- Saji, N.H., Goswami, B.N., Vinayachandran, P.N., Yamagata, T., 1999. A dipole mode in the tropical Indian Ocean. *Nature* 401, 360–363.
- Schär, C., Vidale, P.L., Lüthi, D., Frei, C., Häberli, C., Liniger, M.A., Appenzeller, C., 2004. The role of increasing temperature variability in European summer heatwaves. *Nature* 427, 332–336.
- Schlegel, R.W., Oliver, E.C.J., Wernberg, T., Smit, A.J., 2017. Nearshore and offshore co-occurrence of marine heatwaves and cold-spells. *Prog. Oceanogr.* 151, 189–205.
- Sen Gupta, A., Thomsen, M., Benthuysen, J.A., Hobday, A.J., Oliver, E., Alexander, L.V., Burrows, M.T., Donat, M.G., Feng, M., Holbrook, N.J., Perkins-Kirkpatrick, S., Moore, P.J., Rodrigues, R.R., Scannell, H.A., Taschetto, A.S., Ummenhofer, C.C., Wernberg, T., Smale, D.A., 2020. Drivers and impacts of the most extreme marine heatwave events. *Sci. Rep.* 10.
- Sippo, J.Z., Lovelock, C.E., Santos, I.R., Sanders, C.J., Maher, D.T., 2018. Mangrove mortality in a changing climate: an overview. *Estuar. Coast Shelf Sci.* 215, 241–249.
- Smale, D.A., Wernberg, T., Oliver, E.C.J., Thomsen, M., Harvey, B.P., Straub, S.C., Burrows, M.T., Alexander, L.V., Benthuysen, J.A., Donat, M.G., Feng, M., Hobday, A.J., Holbrook, N.J., Perkins-Kirkpatrick, S.E., Scannell, H.A., Sen Gupta, A., Payne, B.L., Moore, P.J., 2019. Marine heatwaves threaten global biodiversity and the provision of ecosystem services. *Nat. Clim. Change* 9, 306–312.
- Sparnocchia, S., Schiano, M.E., Picco, P., Bozzano, R., Cappelletti, A., 2006. The anomalous warming of summer 2003 in the surface layer of the Central Ligurian Sea (Western Mediterranean). *Ann. Geophys.* 24, 443–452.
- Sprintall, J., Wijffels, S., Molcard, R., Jaya, I., 2010. Direct evidence of the south Java current system in Ombai strait. *Dynam. Atmos. Oceans* 50, 140–156.
- Suadi, Kusano, E., 2019. In: Kusano, Eiichi (Ed.), *Food Value Chain in ASEAN: Case Studies Focusing on Local Producers*, ERIA Research Project Report FY2018 no.5. ERIA, Jakarta, pp. 134–163.
- Susanto, R.D., Gordon, A.L., Zheng, Q., 2001. Upwelling along the coasts of Java and Sumatra and its relation to ENSO. *Geophys. Res. Lett.* 28, 1599–1602.
- Syahputra, A.F., Chen, S., Sujarwo, S., 2020. Superior fishing commodities in southcoast of East Java, Indonesia. *Agric. Socio-Economics J.* 20, 1–6.
- Wernberg, T., Bennett, S., Babcock, R.C., de Bettignies, T., Cure, K., Depczynski, M., Dufois, F., Fromont, J., Fulton, C.J., Hovey, R.K., Harvey, E.S., Holmes, T.H., Kendrick, G.A., Radford, B., Santana-Garcon, J., Saunders, B.J., Smale, D.A., Thomsen, M.S., Tuckett, C.A., Tuya, F., Vanderklift, M.A., Wilson, S., 2016. Climate-driven regime shift of a temperate marine ecosystem. *Science* (80–) 353, 169–172.
- Xie, S.-P., Hu, K., Hafner, J., Tokinaga, H., Du, Y., Huang, G., Sampe, T., 2009. Indian ocean capacitor effect on Indo-western Pacific climate during the summer following El Niño. *J. Clim.* 22, 730–747.
- Xie, S.-P., Kosaka, Y., Du, Y., Hu, K., Chowdary, J.S., Huang, G., 2016. Indo-western Pacific ocean capacitor and coherent climate anomalies in post-ENSO summer: a review. *Adv. Atmos. Sci.* 33, 411–432.
- Zhang, N., Feng, M., Hendon, H.H., Hobday, A.J., Zinke, J., 2017. Opposite polarities of ENSO drive distinct patterns of coral bleaching potentials in the southeast Indian Ocean. *Sci. Rep.* 7, 2443.